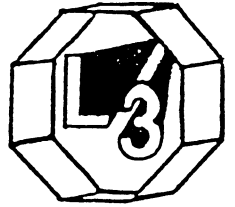CERN-L3 022

A Measurement of the $Z^0 \to b\bar{b}$ Forward-Backward Asymmetry

The L3 Collaboration

ABSTRACT

We have measured the forward-backward asymmetry in $Z^0 \to b\bar{b}$ decays using hadronic events containing muons and electrons. The data sample corresponds to 118,200 hadronic events at $\sqrt{s} \approx M_Z$. From a fit to the single and dilepton p and $p_\perp$ spectra, we determine $A_{b\bar{b}} = 0.130 \, ^{+0.044}_{-0.042}$ including the correction for B^0-$\bar{B}^0$ mixing.

INTRODUCTION

The forward-backward asymmetry of $b\bar{b}$ pairs, $A_{b\bar{b}}$, produced in Z^0 decays is sensitive to the electroweak mixing angle $\sin^2\theta_W$ which is one of the fundamental parameters of the Standard Model.[1-3] We use leptons from the semileptonic decay of one (or both) of the b quarks to select events coming from $Z^0 \to b\bar{b}$. Because of the hard fragmentation and large mass of the b quark, these leptons have large momentum p and large transverse momentum $p_\perp$ with respect to the quark direction. Therefore, we are able to separate $b\bar{b}$ events from events originating from the lighter quarks. As the charge of the lepton is correlated with the charge of the quark, we can use these inclusive leptons to measure $A_{b\bar{b}}$. We use the thrust axis of the event to give the direction of the b or $\bar{b}$ quark, and tag its charge with the lepton charge. We perform a maximum likelihood fit to the single and dilepton p and $p_\perp$ spectra to determine the observed forward-backward asymmetry $A_{b\bar{b}}^{obs}$, taking into account backgrounds coming from charm decays, cascade decays $b \to c \to \ell$, and other background processes. Due to mixing in the B^0-$\bar{B}^0$ system, the observed asymmetry $A_{b\bar{b}}^{obs}$ is smaller than the actual asymmetry $A_{b\bar{b}}$ by a factor $(1 - 2\chi_B)$, where χ_B is the probability that a hadron containing a b quark has oscillated into a hadron containing a $\bar{b}$ quark at the time of its decay. We have reported a measurement of χ_B in a previous paper.[4] Similar techniques have been used to measure $\Gamma_{b\bar{b}}$ and $A_{b\bar{b}}$ with lower statistics.[5,6]

The data sample corresponds to 5.5 pb^{-1} collected during a scan of the Z^0 resonance using the L3 detector at LEP. The center-of-mass energies are distributed over the range $88.2 \leq \sqrt{s} \leq 94.2$ GeV.

THE L3 DETECTOR

The L3 detector covers 99% of 4π. The detector consists of a central tracking chamber, a high resolution electromagnetic calorimeter composed of BGO crystals, a ring of scintillation counters, a uranium and brass hadron calorimeter with proportional wire chamber readout, and an accurate muon chamber system. These detectors are installed in a 12 m diameter magnet which provides a uniform field of 0.5 T along the beam direction.

The central tracking chamber is a time expansion chamber which consists of two cylindrical layers of 12 and 24 sectors, with 62 wires measuring the R-ϕ coordinate. The single wire resolution is 58 μm averaged over the entire cell. The double-track resolution is 640 μm. The fine segmentation of the BGO detector and the hadron calorimeter allow us to measure the direction of jets with an angular resolution of 2.5°, and to measure the total energy of hadronic events from Z^0 decay with a resolution of 10.2%. The muon detector consists of 3 layers of precise drift chambers, which measure a muon's trajectory 56 times in the bending plane, and 8 times in the non-bending direction.

For the present analysis, we use the data collected in the following ranges of polar angles:

- for the central chamber, $41° < \theta < 139°$,

- for the hadron calorimeter, $5° < \theta < 175°$,

- for the muon chambers, $35.8° < \theta < 144.2°$,

- for the electromagnetic calorimeter, $42.4° < \theta < 137.6°$.

A detailed description of each detector subsystem, and its performance, is given in Reference 7.

SELECTION OF $b\bar{b}$ EVENTS

Events of the type $Z^0 \rightarrow b\bar{b}$ are identified by the observation of a hadronic event containing a lepton coming from the semileptonic decay of the b or $\bar{b}$ quark. These inclusive lepton events are triggered by several independent triggers. The primary trigger requires a total energy of 15 GeV in the BGO and hadron calorimeters. A second trigger for inclusive muon events requires one of sixteen barrel scintillation counters in coincidence with a track in the muon chambers. These triggers, combined with an independent charged track trigger and a barrel scintillation counter trigger, give a trigger efficiency greater than 99.9% for hadronic events containing one or more leptons.

In this analysis we first select hadronic events using the following criteria:

(1) $E_{cal} > 38$ GeV,

(2) Relative longitudinal energy imbalance: $\frac{|E_\parallel|}{E_{vis}} < 0.4$,

(3) Relative transverse energy imbalance: $\frac{E_\perp}{E_{vis}} < 0.5$,

where E_{cal} is the total energy observed in the calorimeters, E_{vis} is the sum of the calorimetric energy and the energy of the muon as measured in the muon chambers, and $E_\parallel$ and $E_\perp$ are the energy imbalances parallel and transverse to the beam direction.

The number of jets is found using a two step algorithm which groups the energy deposited in the BGO crystals and in the hadron calorimeter towers into clusters, before collecting the clusters into jets.[8] We require that there be at least one jet which has more than 10 GeV in the calorimeters.

The clustering algorithm normally reconstructs one cluster in the BGO for each electron or photon shower, and a few clusters for τ's. We reject $\tau^+\tau^-$ events by requiring at least 10 clusters in the BGO, each with energy greater than 100 MeV.

A total of 118,200 hadronic events collected during the scan of the Z^0 in the 1989 and 1990 running periods are used for the inclusive muon analysis. For the inclusive electron analysis only the data from 1990 is used, which corresponds to 104,400 hadronic events.

Muons are identified and measured in the muon chamber system. We require that a muon track consists of track segments in at least two of the three layers of muon chambers, and that the muon track points to the interaction region. To

be used in this analysis, the momentum of the muon must be larger than 4 GeV. Charge confusion is negligible for muon candidates in this sample ($\ll 1\%$).

Electrons are identified using the BGO and hadron calorimeters and the tracking chamber. We require a cluster in the BGO whose lateral shower shape is consistent with an electromagnetic shower. The energy in the hadron calorimeter behind this cluster should be small. In addition, the centroid of the cluster must be matched to a track in the chamber. The identification of electrons is described in more detail in Reference 4. To be used in this analysis, the energy of the electron must be larger than 3 GeV. Charge confusion is less than 1% in this sample. Table 1 shows the number of single and dilepton events obtained after all cuts.

Type	Events	Momentum cut
$\mu + hadrons$	5351	$p_\mu > 4$ GeV
$e + hadrons$	1130	$p_e > 3$ GeV
$\mu\mu + hadrons$	229	$p_\mu > 4$ GeV
$ee + hadrons$	21	$p_e > 3$ GeV
$\mu e + hadrons$	111	$p_\mu > 4$ GeV; $p_e > 3$ GeV

Table 1: Number of inclusive lepton events

To determine the acceptance for inclusive lepton events, we use the Lund parton shower program JETSET 7.2[9] with $\Lambda_{LL} = 290$ MeV and string fragmentation. For b and c quarks we use the Peterson fragmentation function.[10] For b quarks, the fragmentation function is adjusted to match our inclusive muon data.[5] The generated events are passed through the L3 detector simulation,[11] which includes the effects of energy loss, multiple scattering, interactions and decays in the detector materials and beam pipe. We use the average of the semileptonic branching ratios measured by previous experiments.[12] $Br(b \to \mu + X) = (11.8 \pm 1.1)\%$ and $Br(c \to \mu + X) = (8.0 \pm 1.0)\%$. These branching ratios are also used for $b \to eX$ and $c \to eX$. We determine that the efficiency for observing a prompt $b \to \ell$ decay is 39.4% for muons and 17.4% for electrons. The lower efficiency for electrons is due to the identification criteria, which require the electron to be isolated.

Figure 1 shows the momentum spectrum for inclusive muons and the energy spectrum for inclusive electrons passing the selection cuts given above. Figure 2 shows the measured transverse momentum, $p_\perp$, of each lepton with respect to the nearest jet. In defining the axis of the nearest jet, the measured energy of the lepton is first excluded from the jet. If there is no jet with an energy greater than 6 GeV remaining in the same hemisphere as the lepton, then $p_\perp$ is calculated relative to the thrust axis of the event. As can be seen from the Monte Carlo distributions also shown in these figures, the fraction of prompt $b \to \ell$ events increases at higher p and $p_\perp$.

Monte Carlo events with leptons are classified into six categories: prompt $b \to \ell$, the cascades $b \to c \to \ell$, $b \to \tau \to \ell$, and $b \to c + \bar{c} + s$ where $\bar{c} \to \ell$, prompt $c \to \ell$, and background. Included in the background are leptons from π and K decays, including Dalitz decays, and mis-identified hadrons caused by, for example, $\pi - \gamma$ overlap for electrons and punchthrough for muons. Table 2 shows the results of Monte Carlo studies giving the fraction of each source of leptons and background for data samples with no cut on $p_\perp$ and also with a cut at 1.5 GeV.

Category	μ $p > 4$ GeV		e $p > 3$ GeV	
	$p_\perp > 0$	$p_\perp > 1.5$	$p_\perp > 0$	$p_\perp > 1.5$
1: $b \to \ell$	38.1%	77.9%	66.8%	84.3%
2: $b \to c \to \ell$	12.0%	4.7%	6.5%	2.5%
3: $b \to \tau \to \ell$	2.1%	1.5%	2.1%	1.7%
4: $b \to \bar{c} \to \ell$	1.9%	0.6%	0.3%	0.1%
5: $c \to \ell$	17.5%	4.7%	3.9%	1.2%
6: background	28.4%	10.6%	20.4%	10.2%

Table 2: Monte Carlo estimates of the fractions of each type of lepton in the data sample.

Rather than using only the data with a high $p_\perp$ cut to determine $A_{b\bar{b}}$, we use a maximum likelihood fitting procedure which gives events with high p and $p_\perp$ larger weights than events with low p or $p_\perp$. This allows us to use the full statistics, while increasing the sensitivity to prompt $b \to \ell$ events.

DETERMINATION OF $A_{b\bar{b}}$

In a semileptonic decay of a b quark, the charge of the detected lepton is directly correlated with the charge of the b (or $\bar{b}$) quark. Using the thrust axis to define the direction of the original quarks and the sign of the lepton charge to distinguish b $(\to \ell^-)$ and $\bar{b}$ $(\to \ell^+)$, we are able to measure the forward-backward asymmetry $A_{b\bar{b}}$ for the process $e^+e^- \to b\bar{b}$. In order to measure this asymmetry, we perform an unbinned maximum likelihood fit to the p versus $p_\perp$ distributions for both single lepton and dilepton events in the data, where we assume no B^0-$\bar{B}^0$ mixing. We then correct $A_{b\bar{b}}^{obs}$ for the effect of mixing.

For single lepton events, the likelihood function is determined from the number and type of the Monte Carlo generated leptons found within a rectangular box centered on each data lepton in the $p - p_\perp$ plane. We allow the size of the box to increase until a minimum number of Monte Carlo leptons are included inside the

box. We require a minimum of 40 leptons in the box. The likelihood function (L) for single lepton events has the form:

$$L = \prod_{i=1}^{N_{data}} \frac{1}{V_{box}(i)} \sum_{k=1}^{6} N_k(i) W_k(i),$$ (1)

where

$$W_k(i) = \frac{1}{2}[1 + A_k f(\theta_i)].$$ (2)

The index k indicates the category of the lepton source type, $N_k(i)$ is the number of simulated Monte Carlo leptons of this category found in the box with data lepton i, and $V_{box}(i)$ is the area of the box. The parameter A_k is the asymmetry associated with each source of leptons. The function $f(\theta_i)$ is the angular dependence of the asymmetry,

$$f(\theta_i) = \left(\frac{8}{3}\right) \frac{\cos(\theta_i)}{1 + \cos^2(\theta_i)},$$ (3)

where θ_i is the polar angle of the thrust axis of the data event with respect to the e^- beam direction. The thrust axis is chosen to point along the b quark direction, as indicated by the lepton charge. Since θ_i is taken from the data, the fit does not rely upon the Monte Carlo description of the $\cos(\theta)$ distribution or the $b\bar{b}$ asymmetry in the Monte Carlo.

The asymmetries, A_k, for the different lepton sources are

$$A_1 = A_{b\bar{b}} \qquad \text{for } b \to \ell,$$
$$A_2 = -A_{b\bar{b}} \qquad \text{for } b \to c \to \ell,$$
$$A_3 = A_{b\bar{b}} \qquad \text{for } b \to \tau \to \ell,$$
$$A_4 = A_{b\bar{b}} \qquad \text{for } b \to \bar{c} \to \ell,$$
$$A_5 = -A_{c\bar{c}} \qquad \text{for } c \to \ell,$$
$$A_6 = A_{back} \qquad \text{for background.}$$

For dilepton events, the fitting procedure is similar, except that we fit in four dimensional $(p_1, p_{\perp 1}, p_2, p_{\perp 2})$ space. The weighting functions are as in Reference 4, modified to include the angular dependence of the asymmetry. We use the average asymmetry of the two leptons, since they are usually from the same primary source.

RESULTS

The result of the fit, which assumes no mixing, is

$$A_{b\bar{b}}^{obs} = 0.084 \pm 0.025.$$

In this fit, the forward-backward asymmetry for primary charm quarks is fixed as a fraction of the b quark asymmetry, $A_{c\bar{c}} = 0.7A_{b\bar{b}}$, and the asymmetry of the background is assumed to be zero. The statistical error of 0.025 includes 0.005 added in quadrature to account for fluctuations in the asymmetry of these background processes. Separate fits to the electron and muon data yield $A_{b\bar{b}}^{obs} = 0.104 \pm 0.029$ for muons, and 0.028 ± 0.044 for electrons.

Our value of $A_{b\bar{b}}^{obs}$ is determined using our entire data sample. In our energy range, the asymmetry is expected to increase as a function of center-of-mass energy. By considering the effects of initial state radiative corrections,[13] we compute that the weighted average center-of-mass energy corresponding to our data sample is 91.28 GeV. Table 4 shows the values of the asymmetry for the data below, on, and above the Z^0 peak.

Mean Energy	$A_{b\bar{b}}^{obs}$
89.63 GeV	0.112 ± 0.057
91.28 GeV	0.061 ± 0.028
93.03 GeV	0.069 ± 0.047

Table 4: $A_{b\bar{b}}^{obs}$ for different center-of-mass energies.

As a consistency check, Figure 3 shows the acceptance corrected angular distribution of the measured b quark direction, for the electron and muon data with $p_{\perp} > 1.5$ GeV. With this cut the sample is approximately 80% pure $b \to \ell$ (see Table 2). The remaining background from cascade $b \to c \to \ell$, charm and the lighter quarks has been subtracted. The curve shows the expected distribution for $A_{b\bar{b}}^{obs} = 0.084$. We note that this acceptance corrected distribution is not used in the fit.

The observed asymmetry must be corrected for the effects of mixing, $A_{b\bar{b}} = A_{b\bar{b}}^{obs}/(1 - 2\chi_B)$. Using our measured value of χ_B,[4] $\chi_B = 0.178^{+0.049}_{-0.040}$, we obtain

$$A_{b\bar{b}} = 0.130^{+0.044}_{-0.042}.$$

Table 5 lists the contributions to the systematic error in this measurement. We have estimated the error by changing several parameters by at least one standard deviation of their known (or estimated) uncertainties. Since the fraction of $c\bar{c}$ events

is small, our measurement of $A_{b\bar{b}}$ is not sensitive to the value of $A_{c\bar{c}}$. We have estimated the effect of reconstruction errors by smearing the transverse momentum of each lepton by 25%. The error coming from the uncertainty in assigning probabilities to events has been estimated by changing the number of leptons required in the fit box, as well as by using different samples of Monte Carlo events. The combined systematic error is estimated to be 0.02.

Contribution	Error
changing the $b \to \ell$ and $c \to \ell$ branching ratios their associated errors	0.006
varying the background fraction by 15%	0.006
varying $A_{c\bar{c}}$ between 0.0 and 0.12	0.006
varying the b fragmentation parameter ϵ_b by $\pm 50\%$	0.007
smearing the lepton transverse momentum by $\Delta p_\perp / p_\perp = 25\%$	0.006
introduction of an additional charge confusion of 0.5%	0.003
probability assignment	0.007
systematic error in χ_B (0.02)	0.007

Table 5: Systematic errors in the $A_{b\bar{b}}$ measurement

We have also performed a fit to simultaneously determine $A_{b\bar{b}}$ and χ_B taking into account correlations between these quantities. Our result is identical to those from the above fit and from Reference 4, both for central values and errors.

DETERMINATION OF $\sin^2 \bar{\theta}_W$

In the Standard Model using the improved Born approximation framework,[1] the forward-backward asymmetry for $Z^0 \to b\bar{b}$ on the peak is given by

$$A_{b\bar{b}}^{Born} = \frac{3}{4} A_e A_b, \tag{4}$$

where

$$A_i = \frac{2 v_i a_i}{v_i^2 + a_i^2} = \frac{2(1 - 4 \mid Q_i \mid \sin^2 \bar{\theta}_W)}{1 + (1 - 4 \mid Q_i \mid \sin^2 \bar{\theta}_W)^2}. \tag{5}$$

Here v_i, a_i and Q_i are the vector and axial-vector coupling constants and the charge of the electron and b quark, and $\sin^2 \bar{\theta}_W$ is the effective weak mixing angle. To compare our measured asymmetry to this Born level calculation, QED and QCD

corrections and the shift between the Z^0 mass and our effective center-of-mass energy must be taken into account.[*] To do this we use the formulation given in Reference 1. We obtain

$$\sin^2 \bar{\theta}_W = 0.226 \pm 0.008.$$

This value can be compared with the prediction of the Standard Model for a top-quark mass of 130 GeV[14] and Higgs mass of 100 GeV of $\sin^2 \bar{\theta}_W = 0.233$.

CONCLUSIONS

We have analyzed $Z^0 \to b\bar{b}$ decays using inclusive lepton events selected from a sample of 118,200 hadronic events. From a fit to the p and $p_\perp$ distributions for single lepton and dilepton events, we have determined the $b\bar{b}$ forward-backward charge asymmetry at $\sqrt{s} \approx M_Z$. Near the Z^0 peak, the $b\bar{b}$ asymmetry is $A_{b\bar{b}} = 0.130 \, ^{+0.044}_{-0.042}$, where the errors are statistical only. From this measurement we determine $\sin^2 \bar{\theta}_W$ to be 0.226 ± 0.008.

ACKNOWLEDGMENTS

---

[*] In principle, the coupling constants for the b quark need additional corrections depending on the mass of the top quark. However, as the corrections appear in both the numerator and denominator of Eqn. (5), they almost completely cancel.

The L3 Collaboration:

B.Adeva[15] O.Adriani[13] M.Aguilar-Benitez[23] H.Akbari[5] J.Alcaraz[23] A.Aloisio[25] G.Alverson[9]
M.G.Alviggi[25] Q.An[16] H.Anderhub[39] A.L.Anderson[12] V.P.Andreev[14] T.Angelov[12] L.Antonov[34]
D.Antreasyan[7] P.Arce[23] A.Arefiev[24] T.Azemoon[3] T.Aziz[8] P.V.K.S.Baba[16] P.Bagnaia[30] J.A.Bakken[29]
L.Baksay[32] R.C.Ball[3] S.Banerjee[8,16] J.Bao[5] L.Barone[30] A.Bay[17] U.Becker[12] J.Behrens[39] S.Beingessner[4]
Gy.L.Bencze[10] J.Berdugo[23] P.Berges[12] B.Bertucci[30] B.L.Betev[34] A.Biland[39] R.Bizzarri[30] J.J.Blaising[4]
P.Blömeke[1] B.Blumenfeld[5] G.J.Bobbink[2] M.Bocciolini[13] W.Böhlen[37] A.Böhm[1] T.Böhringer[19]
B.Borgia[30] D.Bourilkov[34] M.Bourquin[17] D.Boutigny[4] B.Bouwens[2] J.G.Branson[31] I.C.Brock[28]
F.Bruyant[15] C.Buisson[22] A.Bujak[36] J.D.Burger[12] J.P.Burq[22] J.Busenitz[35] X.D.Cai[16] C.Camps[1]
M.Capell[20] F.Carbonara[25] F.Carminati[13] A.M.Cartacci[13] M.Cerrada[23] F.Cesaroni[30] Y.H.Chang[12]
U.K.Chaturvedi[16] M.Chemarin[22] A.Chen[41] C.Chen[6] G.M.Chen[6] H.F.Chen[18] H.S.Chen[6] M.Chen[12]
M.C.Chen[27] M.L.Chen[3] G.Chiefari[25] C.Y.Chien[5] F.Chollet[4] C.Civinini[13] I.Clare[12] R.Clare[12]
H.O.Cohn[26] G.Coignet[4] N.Colino[15] V.Commichau[1] G.Conforto[13] A.Contin[15] F.Crijns[2] X.Y.Cui[16]
T.S.Dai[12] R.D'Alessandro[13] R.de Asmundis[25] A.Degré[15,4] K.Deiters[15,38] E.Dénes[10] P.Denes[29]
F.DeNotaristefani[30] M.Dhina[39] D.DiBitonto[35] M.Diemoz[30] F.Diez-Hedo[15] H.R.Dimitrov[34] C.Dionisi[30]
F.Dittus[27] R.Dolin[12] E.Drago[25] T.Driever[2] D.Duchesneau[17] P.Duinker[2,15] I.Duran[15,23] H.El Mamouni[22]
A.Engler[28] F.J.Eppling[12] F.C.Erné[2] P.Extermann[17] R.Fabbretti[39] G.Faber[12] S.Falciano[30] Q.Fan[16,6]
S.J.Fan[33] M.Fabre[39] O.Fackler[20] J.Fay[22] J.Fehlmann[39] H.Fenker[9] T.Ferguson[28] G.Fernandez[23]
F.Ferroni[30,15] H.Fesefeldt[1] J.Field[17] F.Filthaut[2] G.Finocchiaro[30] P.H.Fisher[5] G.Forconi[17] T.Foreman[2]
K.Freudenreich[39] W.Friebel[38] M.Fukushima[12] M.Gailloud[19] Yu.Galaktionov[24] E.Gallo[13] S.N.Ganguli[8]
P.Garcia-Abia[23] S.S.Gau[41] S.Gentile[30] M.Glaubman[9] S.Goldfarb[3] Z.F.Gong[16,18] E.Gonzalez[23]
A.Gordeev[24] P.Göttlicher[1] D.Goujon[17] G.Gratta[27] C.Grinnell[12] M.Gruenewald[27] M.Guanziroli[16]
A.Gurtu[8] H.R.Gustafson[3] L.J.Gutay[36] H.Haan[1] S.Hancke[1] K.Hangarter[1] M.Harris[15] A.Hasan[16]
D.Hauschildt[2] C.F.He[33] T.Hebbeker[1] M.Hebert[31] G.Herten[12] U.Herten[1] A.Hervé[15] K.Hilgers[1]
H.Hofer[39] H.Hoorani[16] L.S.Hsu[41] G.Hu[16] G.Q.Hu[33] B.Ille[22] M.M.Ilyas[16] V.Innocente[25,15] E.Isiksal[39]
E.Jagel[16] B.N.Jin[6] L.W.Jones[3] R.A.Khan[16] Yu.Kamyshkov[24] Y.Karyotakis[4,15] M.Kaur[16] S.Khokhar[16]
V.Khoze[14] M-N.Kienzle[17] W.Kinnison[21] D.Kirkby[27] W.Kittel[2] A.Klimentov[24] A.C.König[2] O.Kornadt[1]
V.Koutsenko[24] R.W.Kraemer[28] T.Kramer[12] V.R.Krastev[34] W.Krenz[1] J.Krizmanic[5] A.Kuhn[37]
K.S.Kumar[11] V.Kumar[16] A.Kunin[24] A.van Laak[1] V.Lalieu[17] G.Landi[13] K.Lanius[15] D.Lanske[1]
S.Lanzano[25] P.Lebrun[22] P.Lecomte[39] P.Lecoq[15] P.Le Coultre[39] D.Lee[21] I.Leedom[9] J.M.Le Goff[15]
L.Leistam[15] R.Leiste[38] M.Lenti[13] J.Lettry[39] P.M.Levchenko[14] X.Leytens[2] C.Li[18] H.T.Li[6] J.F.Li[16]
L.Li[39] P.J.Li[33] Q.Li[16] X.G.Li[6] J.Y.Liao[33] Z.Y.Lin[18] F.L.Linde[28] D.Linnhofer[15] R.Liu[16] Y.Liu[16]
W.Lohmann[38] S.Lökös[32] E.Longo[30] Y.S.Lu[6] J.M.Lubbers[2] K.Lübelsmeyer[1] C.Luci[15] D.Luckey[7,12]
L.Ludovici[30] X.Lue[39] L.Luminari[30] W.G.Ma[18] M.MacDermott[39] R.Magahiz[32] M.Maire[4] P.K.Malhotra[8]
R.Malik[16] A.Malinin[24] C.Maña[23] D.N.Mao[3] Y.F.Mao[6] M.Maolinbay[39] P.Marchesini[16] A.Marchionni[13]
J.P.Martin[22] L.Martinez[15] F.Marzano[30] G.G.G.Massaro[2] T.Matsuda[12] K.Mazumdar[8] P.McBride[11]
T.McMahon[36] D.McNally[39] Th.Meinholz[1] M.Merk[2] L.Merola[25] M.Meschini[13] W.J.Metzger[2]
Y.Mi[16] M.Micke[1] U.Micke[1] G.B.Mills[21] Y.Mir[16] G.Mirabelli[30] J.Mnich[1] M.Möller[1] B.Monteleoni[13]
G.Morand[17] R.Morand[4] S.Morganti[30] V.Morgunov[24] R.Mount[27] E.Nagy[10] M.Napolitano[25] H.Newman[27]
M.A.Niaz[16] L.Niessen[1] D.Pandoulas[1] F.Plasil[26] G.Passaleva[13] G.Paternoster[25] S.Patricelli[25]
Y.J.Pei[1] D.Perret-Gallix[4] J.Perrier[17] A.Pevsner[5] M.Pieri[13] P.A.Piroué[29] V.Plyaskin[24] M.Pohl[39]
V.Pojidaev[24] N.Produit[17] J.M.Qian[12,16] K.N.Qureshi[16] R.Raghavan[8] G.Rahal-Callot[39] P.Razis[39]
K.Read[29] D.Ren[39] Z.Ren[16] S.Reucroft[9] O.Rind[3] C.Rippich[28] H.A.Rizvi[16] B.P.Roe[3] M.Röhner[1]
S.Röhner[1] U.Roeser[38] Th.Rombach[1] L.Romero[23] J.Rose[1] S.Rosier-Lees[4] R.Rosmalen[2] Ph.Rosselet[19]
J.A.Rubio[15,23] W.Ruckstuhl[17] H.Rykaczewski[39] M.Sachwitz[38] J.Salicio[15,23] J.M.Salicio[23] G.Sanders[21]
G.Sartorelli[7,16] G.Sauvage[4] A.Savin[24] V.Schegelsky[14] D.Schmitz[1] P.Schmitz[1] M.Schneegans[4]
M.Schöntag[1] H.Schopper[40] D.J.Schotanus[2] H.J.Schreiber[38] R.Schulte[1] S.Schulte[1] K.Schultze[1]
J.Schütte[1] J.Schwenke[1] G.Schwering[1] C.Sciacca[25] I.Scott[11] R.Sehgal[16] P.G.Seiler[39] J.C.Sens[2] I.Sheer[31]
V.Shevchenko[24] S.Shevchenko[24] X.R.Shi[28] K.Shmakov[24] V.Shoutko[24] E.Shumilov[24] N.Smirnov[14]
A.Sopczak[27,31] C.Spartiotis[5] T.Spickermann[1] B.Spiess[37] P.Spillantini[13] R.Starosta[1] M.Steuer[7,12]
D.P.Stickland[29] W.Stoeffl[20] B.Stöhr[39] H.Stone[17] K.Strauch[11] B.C.Stringfellow[36] K.Sudhakar[8,1]
G.Sultanov[15] R.L.Sumner[29] L.Z.Sun[18] H.Suter[39] R.B.Sutton[28] J.D.Swain[16] A.A.Syed[16] X.W.Tang[6]
E.Tarkovsky[24] L.Taylor[9] E.Thomas[16] C.Timmermans[2] Samuel C.C.Ting[12] S.M.Ting[12] Y.P.Tong[41]
F.Tonisch[38] M.Tonutti[1] S.C.Tonwar[8] J.Tòth[10] G.Trowitzsch[38] K.L.Tung[6] J.Ulbricht[37] L.Urbàn[10]
U.Uwer[1] E.Valente[30] R.T.Van de Walle[2] H.van der Graaf[2] I.Vetlitsky[24] G.Viertel[39] P.Vikas[16] U.Vikas[16]
M.Vivargent[4,12] H.Vogel[28] H.Vogt[38] M.Vollmar[1] G.Von Dardel[15] I.Vorobiev[24] A.A.Vorobyov[14]
An.A.Vorobyov[14] L.Vuilleumier[19] M.Wadhwa[16] W.Wallraff[1] C.R.Wang[18] G.H.Wang[28] J.H.Wang[6]
Q.F.Wang[11] X.L.Wang[18] Y.F.Wang[13] Z.Wang[16] Z.M.Wang[16,18] J.Weber[39] R.Weill[19] T.J.Wenaus[12]

J.Wenninger[17] M.White[12] R.Wilhelm[2] C.Willmott[23] F.Wittgenstein[15] D.Wright[29] R.J.Wu[6] S.L.Wu[16] S.X.Wu[16] Y.G.Wu[6] B.Wyslouch[12] Y.D.Xu[6] Z.Z.Xu[18] Z.L.Xue[33] D.S.Yan[33] B.Z.Yang[18] C.G.Yang[6] G.Yang[16] K.S.Yang[6] Q.Y.Yang[6] Z.Q.Yang[33] C.H.Ye[16] J.B.Ye[39] Q.Ye[16] S.C.Yeh[41] Z.W.Yin[33] J.M.You[16] M.Yzerman[2] C.Zaccardelli[27] L.Zehnder[39] M.Zeng[16] Y.Zeng[1] D.Zhang[31] D.H.Zhang[2] Z.P.Zhang[18] J.F.Zhou[1] R.Y.Zhu[27] H.L.Zhuang[6] A.Zichichi[15,16]

1 I. Physikalisches Institut, RWTH, Aachen, Federal Republic of Germany[§]
  III. Physikalisches Institut, RWTH, Aachen, Federal Republic of Germany[§]
2 National Institute for High Energy Physics, NIKHEF, Amsterdam; NIKHEF-H and University of Nijmegen, Nijmegen, The Netherlands
3 University of Michigan, Ann Arbor, Michigan, United States of America
4 Laboratoire de Physique des Particules, LAPP, Annecy, France
5 Johns Hopkins University, Baltimore, Maryland, United States of America
6 Institute of High Energy Physics, IHEP, Beijing, China
7 INFN-Sezione di Bologna, Italy
8 Tata Institute of Fundamental Research, Bombay, India
9 Northeastern University, Boston, Massachusetts, United States of America
10 Central Research Institute for Physics of the Hungarian Academy of Sciences, Budapest, Hungary
11 Harvard University, Cambridge, Massachusetts, United States of America
12 Massachusetts Institute of Technology, Cambridge, Massachusetts, United States of America
13 INFN Sezione di Firenze and University of Firenze, Italy
14 Leningrad Nuclear Physics Institute, Gatchina, Soviet Union
15 European Laboratory for Particle Physics, CERN, Geneva, Switzerland
16 World Laboratory, FBLJA Project, Geneva, Switzerland
17 University of Geneva, Geneva, Switzerland
18 Chinese University of Science and Technology, USTC, Hefei, China
19 University of Lausanne, Lausanne, Switzerland
20 Lawrence Livermore National Laboratory, Livermore, California, United States of America
21 Los Alamos National Laboratory, Los Alamos, New Mexico, United States of America
22 Institut de Physique Nucléaire de Lyon, IN2P3-CNRS/Université Claude Bernard, Villeurbanne, France
23 Centro de Investigaciones Energeticas, Medioambientales y Tecnologicas, CIEMAT, Madrid, Spain
24 Institute of Theoretical and Experimental Physics, ITEP, Moscow, Soviet Union
25 INFN-Sezione di Napoli and University of Naples, Italy
26 Oak Ridge National Laboratory, Oak Ridge, Tennessee, United States of America
27 California Institute of Technology, Pasadena, California, United States of America
28 Carnegie Mellon University, Pittsburgh, Pennsylvania, United States of America
29 Princeton University, Princeton, New Jersey, United States of America
30 INFN-Sezione di Roma and University of Roma, "La Sapienza", Italy
31 University of California, San Diego, California, United States of America
32 Union College, Schenectady, New York, United States of America
33 Shanghai Institute of Ceramics, SIC, Shanghai, China
34 Central Laboratory of Automation and Instrumentation, CLANP, Sofia, Bulgaria
35 University of Alabama, Tuscaloosa, Alabama, United States of America
36 Purdue University, West Lafayette, Indiana, United States of America
37 Paul Scherrer Institut, PSI, Würenlingen, Switzerland
38 High Energy Physics Institute, Zeuthen-Berlin, Federal Republic of Germany
39 Eidgenössische Technische Hochschule, ETH Zürich Switzerland
40 University of Hamburg, Federal Republic of Germany
41 High Energy Physics Group, Taiwan, China
§ Supported by the German Bundesministerium für Forschung und Technologie

REFERENCES

1. A. Djouadi *et al.*, *Z. Phys.* **C46** (1990) 411.

2. J. Kühn and P. Zerwas, "Heavy Flavors at LEP," MPI-PAE/PTh 49/89.

3. M. Böhm, W. Hollik, *et al.*, in "Z Physics at LEP I," CERN 89-08, ed. G. Altarelli *et al.*, Vol 1, p 203.

4. L3 Collaboration, B. Adeva *et al.*, "A Measurement of B^0-$\bar{B}^0$ Mixing in Z^0 Decays," L3 Preprint #20, submitted to Phys. Lett. B.

5. L3 Collaboration, B. Adeva *et al.*, *Phys. Lett.* **B 241** (1990) 416.

6. ALEPH Collaboration, D. Decamp *et al.*, *Phys. Lett.* **B 244** (1990) 551; MARK II Collaboration, J. F. Kral *et al.*, *Phys. Rev. Lett.* **64** (1990) 1211.

7. L3 Collaboration, B. Adeva *et al.*, *Nucl. Inst. and Meth.* **A289** (1990) 35.

8. O. Adriani *et al.*, "Hadron Calorimetry in the L3 Detector," to be published in Nuclear Instruments and Methods.

9. T. Sjöstrand and M. Bengtsson, *Comput. Phys. Commun.* **43** (1987) 367; T. Sjöstrand in "Z Physics at LEP," CERN Report CERN-89-08, Vol.III, p. 143.

10. C. Peterson *et al.*, *Phys. Rev.* **D 27** (1983) 105.

11. The L3 detector simulation is based on GEANT Version 3.13, September, 1989. See R. Brun *et al.*, "GEANT 3," CERN DD/EE/84-1 (Revised), September 1987. Hadronic interactions are simulated using the GHEISHA program; see H. Fesefeldt, RWTH Aachen Preprint PITHA 85/02 (1985).

12. The semileptonic branching ratios are taken from PEP and PETRA data. See JADE Collaboration, W. Bartel *et al.*, *Z. Phys.* **C 33** (1987) 339, and references therein.

13. D. Bardin *et al.*, Berlin-Zeuthen preprint PHE-89-19 (1989). See also: J.E. Campagne and R. Zitoun, *Z. Phys.* **C 43** (1989) 469.

14. L3 Collaboration, B. Adeva *et al.*, *Phys. Lett.* **B 249** (1990) 341.

FIGURE CAPTIONS

1. The measured muon momentum (a) and electron energy (b) distributions for inclusive lepton events compared to the Monte Carlo simulation. No $p_\perp$ cut has been applied. The contributions of the various processes are indicated. The data at high momentum are dominated by $b \to \ell$ decays.

2. The measured distributions of the transverse momentum $p_\perp$ of the muon (a) and electron (b) with respect to the nearest jet. Cuts of $p_\mu > 4$ GeV for the muons, and $p_e > 3$ GeV for the electrons have been applied. The contributions of the various processes are indicated. The data at large $p_\perp$ are dominated by $b \to \ell$ decays.

3. The acceptance corrected distribution of the measured b quark direction, $\cos \theta_b$, for the electron and muon data. The thrust axis defines the direction of the quark, and the sign of the lepton charge is used to tag the b or $\bar{b}$ quark. The curve shows the expected distribution for $A_{b\bar{b}}^{obs} = 0.084$. Note that this distribution was not used in the fit.
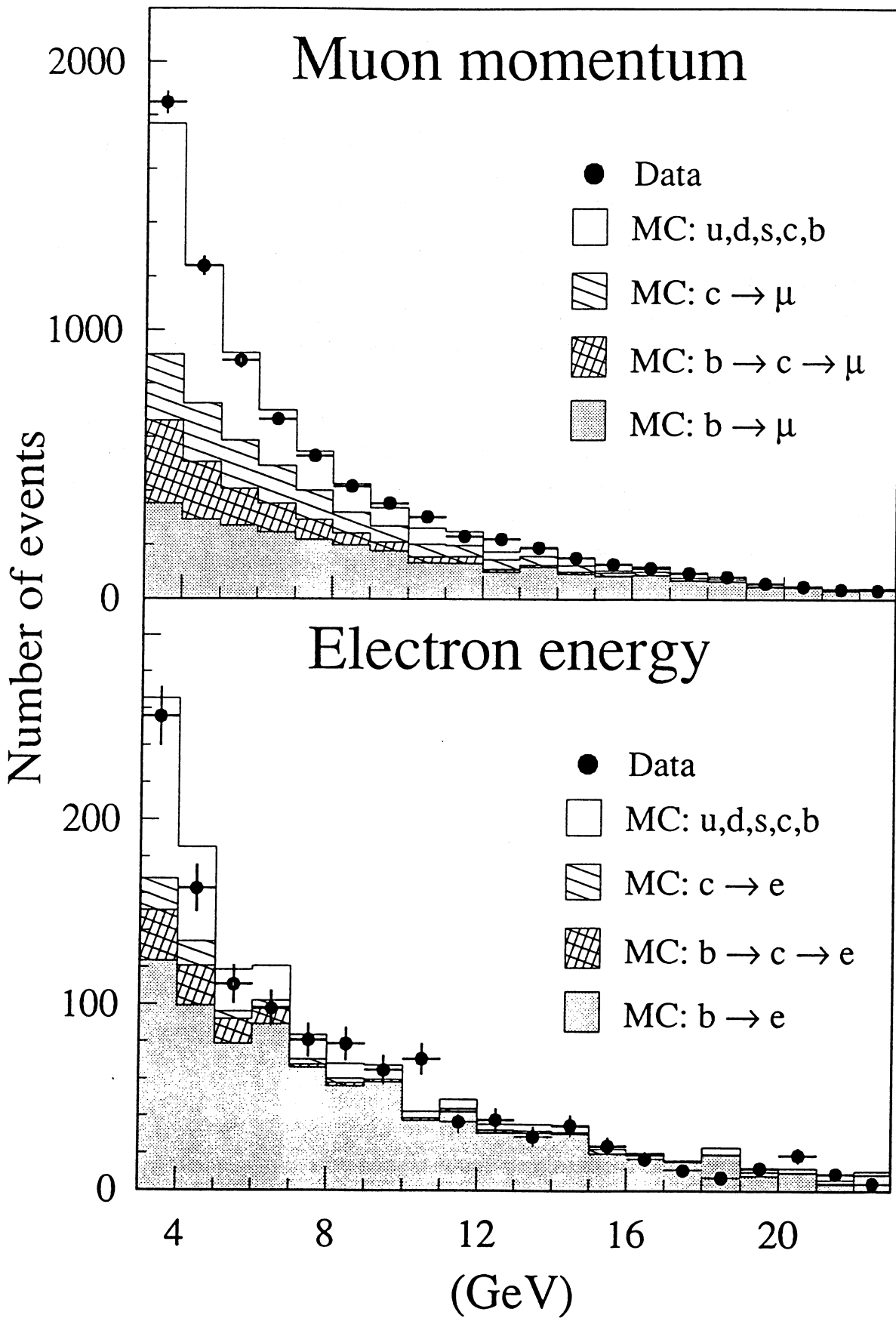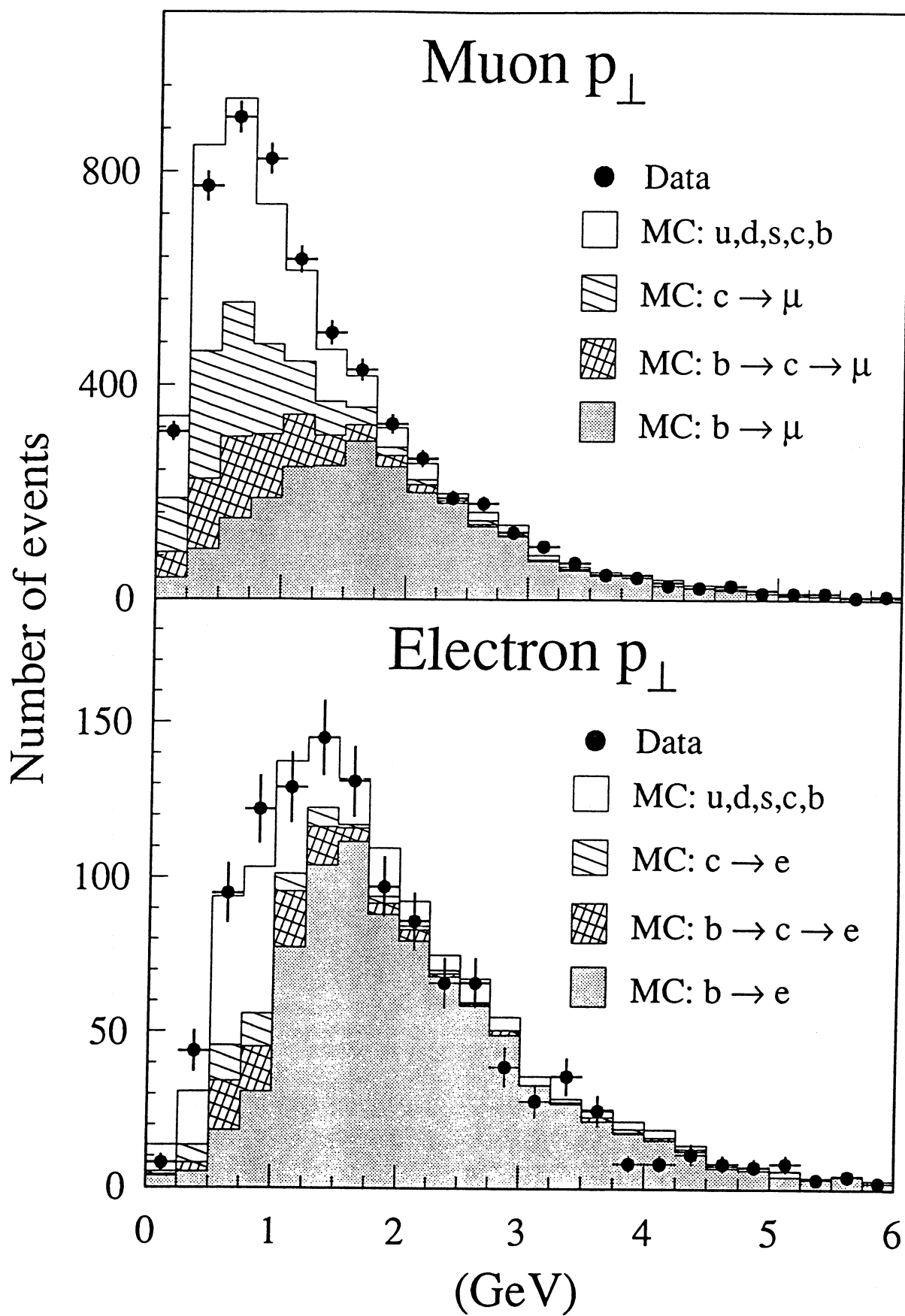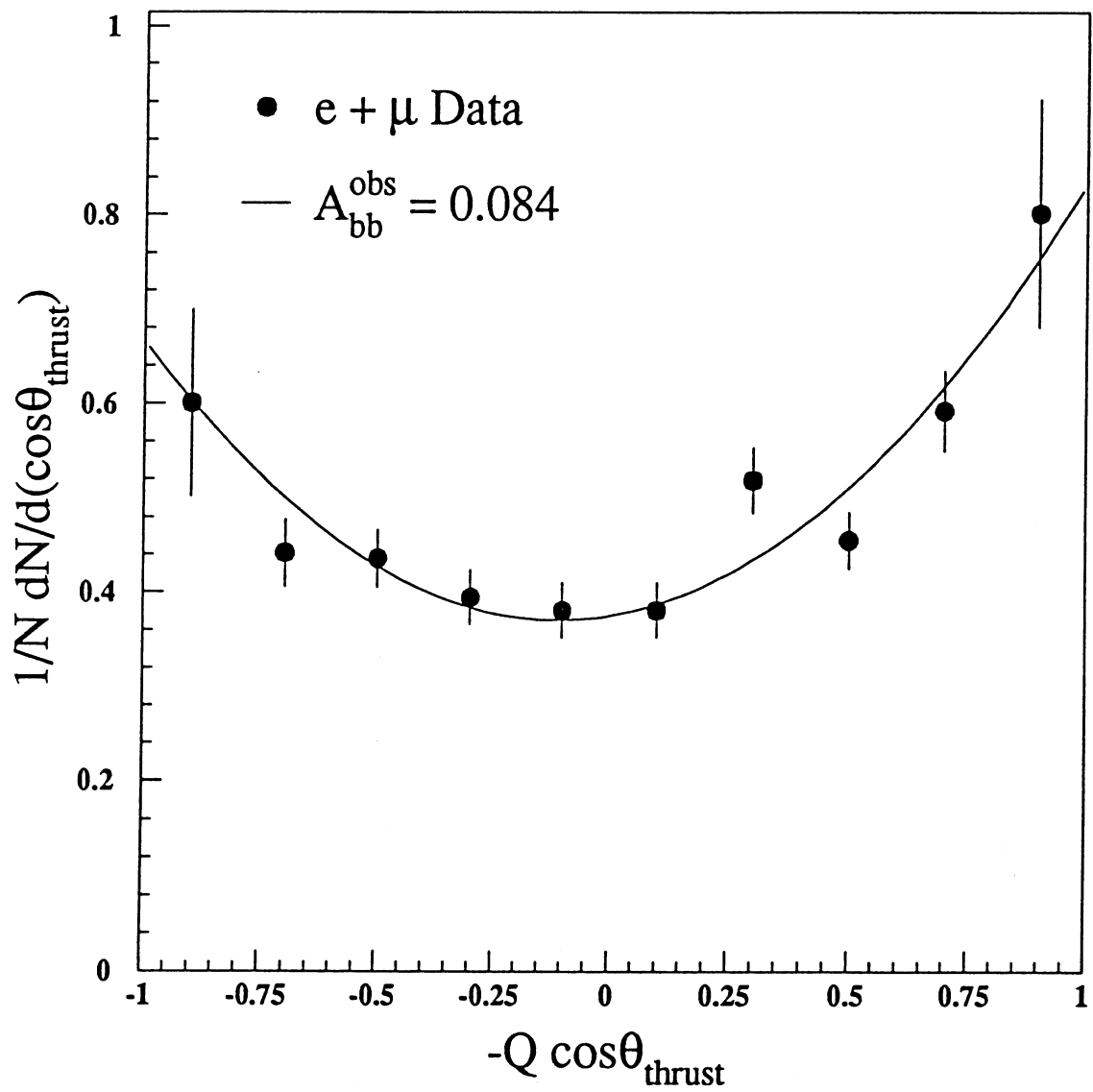
Figure 1

Figure 2

Figure 3